

See discussions, stats, and author profiles for this publication at: <https://www.researchgate.net/publication/304779861>

# A 980 nm driven photothermal ablation of virulent and antibiotic resistant Gram-positive and Gram-negative...

Article in *Journal of Colloid and Interface Science* · July 2016

DOI: 10.1016/j.jcis.2016.07.002

CITATIONS

2

READS

204

10 authors, including:



**Djamel Drider**

Université des Sciences et Technologies de Li...

108 PUBLICATIONS 1,771 CITATIONS

SEE PROFILE



**Julie Bouckaert**

Université des Sciences et Technologies de Li...

134 PUBLICATIONS 2,840 CITATIONS

SEE PROFILE



**Radhouane Chtourou**

Centre des Recherches et des Technologies d...

149 PUBLICATIONS 881 CITATIONS

SEE PROFILE



**Rabah Boukherroub**

French National Centre for Scientific Research

549 PUBLICATIONS 9,864 CITATIONS

SEE PROFILE

Some of the authors of this publication are also working on these related projects:



functionalization of surface [View project](#)



Composites materials [View project](#)



## Regular Article

# A 980 nm driven photothermal ablation of virulent and antibiotic resistant Gram-positive and Gram-negative bacteria strains using Prussian blue nanoparticles



Houcem Maaoui<sup>a,b</sup>, Roxana Jijie<sup>a,c</sup>, Guo-Hui Pan<sup>d</sup>, Djamel Drider<sup>e</sup>, Delphine Caly<sup>e</sup>, Julie Bouckaert<sup>f</sup>, Nicoleta Dumitrascu<sup>c</sup>, Radouane Chtourou<sup>g</sup>, Sabine Szunerits<sup>a</sup>, Rabah Boukherroub<sup>a,\*</sup>

<sup>a</sup> Institut d'Electronique, de Microélectronique et de Nanotechnologie (IEMN, UMR CNRS 8520), Université Lille 1, Avenue Poincaré, BP 60069, 59652 Villeneuve d'Ascq, France

<sup>b</sup> Département de Physique, Faculté des Sciences de Tunis, Université Tunis-El Manar, 2092, Tunisia

<sup>c</sup> Iasi Plasma Advanced Research Center (IPARC), Faculty of Physics, Alexandru Ioan Cuza University of Iasi, Bd. Carol I No. 11, Iasi 700506, Romania

<sup>d</sup> State Key Laboratory of Luminescence and Applications, Changchun Institute of Optics, Fine Mechanics and Physics, Chinese Academy of Sciences, 3888 Dong Nanhu Road, Changchun 130033, China

<sup>e</sup> Université Lille 1, Institut Charles Viollette – EA 7394, Lille, France

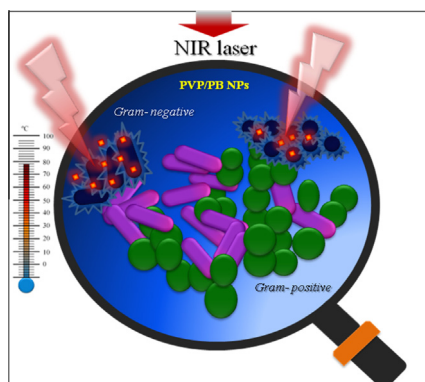
<sup>f</sup> Unité de Glycobiologie Structurale et Fonctionnelle (UGSF), UMR 8576 CNRS, Université de Lille, 59000 Lille, France

<sup>g</sup> Centre des Recherches et des Technologies de l'Energie, B.P. 95, Hammam-Lif 2050, Tunisia

## HIGHLIGHTS

- PVP-coated Prussian blue nanoparticles are used as a photothermal agent.
- The nanoparticles are not cytotoxic to cells under NIR irradiation.
- The nanoparticles are highly efficient for bacteria eradication.

## GRAPHICAL ABSTRACT



## ARTICLE INFO

## Article history:

Received 25 May 2016

Revised 30 June 2016

Accepted 1 July 2016

Available online 2 July 2016

## Keywords:

Prussian blue  
Near infrared  
Photothermal  
Gram positive  
Gram negative  
Bacteria

## ABSTRACT

A 980 nm laser-driven antimicrobial photothermal therapy using poly(vinylpyrrolidone)-coated Prussian Blue nanoparticles (PVP/PB NPs) is demonstrated. This approach allows an efficient eradication of a virulent strain of Gram-negative *Escherichia coli* (*E. coli*) associated with urinary tract infection as well as for the ablation of antibiotic resistant pathogens such as methicillin resistant *Staphylococcus aureus* (MRSA) and extended spectrum  $\beta$ -lactamase (ESBL) *E. coli*. Interestingly the 980 nm irradiation exhibits minimal effect on mammalian cells up to a PVP/PB NPs concentration of  $50 \mu\text{g mL}^{-1}$ , while at this concentration bacteria are completely eradicated. This feature is certainly very promising for the selective targeting of bacteria over mammalian cells.

© 2016 Elsevier Inc. All rights reserved.

\* Corresponding author.

E-mail address: [rabah.boukherroub@univ-lille1.fr](mailto:rabah.boukherroub@univ-lille1.fr) (R. Boukherroub).

## 1. Introduction

The increase of multidrug-resistant bacteria infections has become a major problem in modern healthcare. Indeed, bacteria replicate very rapidly and any mutation that facilitates the survival of the pathogen in the presence of an antibiotic drug will quickly become predominant in the microbial population. The treatment of bacterial infections with multi-resistant germs is extremely difficult, as the development of new antimicrobial drugs is hardly catching up with the development of antibiotic-resistant bacteria [1–3]. Several reports have shown that various nanomaterials could be considered as viable alternative candidates to antibiotics [4–7], which are in addition able to overcome the resistance problem underwent by conventional drugs [8–10]. A different strategy for the inactivation of bacteria is photothermal therapy (PTT), based on the use of strong light-absorbing materials, which upon exposure to laser radiation create local hyperthermic effects. The involvement of near infrared (NIR) light in 700–1100 nm range is of particular interest for PTT, because absorption of NIR photons in biological tissues is minimal and the penetration depth is optimal. The wavelength range of 700–900 nm is considered as a spectral transparent window, exhibiting lower absorbance and scattering by molecules like melanin and hemoglobin [11]. The wavelength of 980 nm, widely used in the construction of biomedical lasers, does not fall within this range due to the onset of the vibration of water molecules with consequently higher absorption cross section. However, the absorption by water molecules at 980 nm is not causing problems in most cases [12,13]. The advantage of PTT at 980 nm excitation is associated with deeper tissue penetration and a low level degradation of biomolecules and cellular photodamage.

Urinary tract infections (UTI) caused by *Escherichia coli* (*E. coli*) present a major economic and societal burden. The practiced and therapeutics proposed for UTI management include the prophylactic and phytotherapy treatments, and the use of vaccination or drug therapies [14]. It is well-known that antibiotics resistance in bacteria has developed at an accelerated rate due to pathogenic adaptation. Today, extended spectrum  $\beta$ -lactamase-producing (ESBL) *E. coli* [15] and methicillin-resistant *Staphylococcus aureus* (MRSA) became significant threats in both health care-associated and community-associated infections. Research aiming at the management of the most common clinical syndromes encountered by adult and pediatric clinicians who care for patients with MRSA infections has been reported [15,16].

Here, we describe an interesting finding that polyvinylpyrrolidone coated Prussian blue nanoparticles (PVP/PB NPs) allow effective photothermal ablation of bacteria at 810 or 980 nm. PB-based nanostructures, clinically approved agents which can be produced at low cost and large quantities, proved to be efficient PTT agents due to their high optical absorbance peak at  $\sim$ 700 nm. PB NPs have thus been explored in the last few years as PTT agent for cancer treatment [17–24]. In contrast to gold nanorods, the NIR absorption is derived from charge transfer transition between Fe(II) and Fe(III) instead of localized surface plasmon resonance, providing PB NPs with improved photothermal stability. Although, the efficacy of PB NPs for cancer cells killing has been demonstrated, there is no report on the utilization of such a nanosystem for the PTT bacteria ablation. In this work, we demonstrate the high potential of PB NPs upon laser irradiation at 810 or 980 nm for the eradication of Gram-positive and Gram-negative pathogens.

## 2. Experimental section

### 2.1. Materials

Hydrochloric acid (HCl), Potassium hexacyanoferrate(III) [ $K_3Fe(CN)_6$ ], polyvinylpyrrolidone (PVP10, average  $M_w$  10,000) were

obtained from Sigma-Aldrich and used without any further purification.

### 2.2. Preparation of PVP-coated Prussian blue nanoparticles (PVP/PB NPs)

The PVP/PB NPs investigated in this work were synthesized by addition of PVP (1 g) and potassium ferrocyanide (0.2 g) to an aqueous solution (20 mL, pH = 2 adjusted with HCl) [25]. After 30 min of stirring, a clear solution was obtained, which was aged at 80 °C for 3 h. The resulting precipitate was collected by centrifugation, washed in distilled water and ethanol several times and dried at 100 °C for 12 h.

### 2.3. Characterization

Powder X-ray diffraction (XRD) patterns were collected on a Bruker D8 advance diffractometer (Cu-K $\alpha$  radiation, 1.54056 Å) with an applied voltage of 40 kV and an anode current of 40 mA in the  $2\theta$  range of 10–80°.

Transmission electron microscopy (TEM) and high resolution TEM (HRTEM) images were acquired using a FEI Tecnai G<sup>2</sup>-F20 transmission electron microscope operating at an acceleration voltage of 200 kV. The samples were drop-coated from ethanolic dispersion of PVP/PB NPs onto carbon-coated copper TEM grids and the solvent was evaporated under ambient conditions.

UV/Vis Absorption spectra were recorded using a Perkin Elmer Lambda UV/Vis 950 spectrophotometer in quartz cuvettes with an optical path of 10 mm. The wavelength range was 200–1100 nm.

### 2.4. Measurement of the photothermal effect

All irradiations were performed in standard 96-well plates. The temperature changes were captured by an Infrared Camera (Thermovision A40) and treated using ThermoCam Researcher Pro 2.9 software. A 810/980 nm-CW LASER (Gbox model, Fournier Medical Solution, France) was used for the photothermal experiments. This laser was injected into a 400 mm core fibre which output was placed around 6 cm away from the bottom of the wells. This output was not collimated and the resulting beam divergence allowed us to illuminate uniformly up to 4 wells.

### 2.5. Cytotoxicity assay

The HeLa cell line was cultured and maintained in Dulbecco's Modified Eagle's medium (DMEM, Gibco<sup>®</sup>) supplemented with 10% fetal bovine serum (FBS, Gibco<sup>®</sup>) and 1% penicillin-streptomycin (Gibco<sup>®</sup>) in a humidified incubator at 37 °C and 5% CO<sub>2</sub>. HeLa cells were seeded at a density of 10<sup>4</sup> cells/well in a 96-well plate and grown for 48 h before assay. The culture medium was replaced with a fresh medium that contains the PVP/PB nanoparticles at different concentrations. After 24 h, the old medium was aspirated and cells were washed three times with PBS. The cell viability was evaluated using Cell Counting Kit-8 (CCK-8, Sigma Aldrich) assay. Briefly, 10  $\mu$ L of the CCK-8 solution were added to each well containing 100  $\mu$ L of DMEM with 10% FBS and the plate was incubated for 3 h in the humidified incubator. The absorbance of each well at 450 nm was measured using a microplate reader (PHERAstar FS, BMG LABTECH GmbH, Germany). Each condition was replicated five times and the mean absorbance value of non-exposed cells was taken as 100% cellular viability.

## 2.6. Photothermal ablation of cells

HeLa cells were seeded in 96 well plates (100  $\mu\text{L}$ , DMEM) at a density of  $5 \times 10^4$  cells per well 24 h before assay. PVP/PB NPs were added at different concentrations and the wells were irradiated at 810 or 980 nm for 10 min at  $1 \text{ W cm}^{-2}$ . Cell viability was evaluated using the CCK-8 assay, where the absorbance at 450 nm is measured using a microplate reader, as above.

## 2.7. Photothermal ablation of bacteria

The reference strains uropathogenic *E. coli* UTI89 and the ESBL-producing *E. coli* isolate S5 were grown at  $37^\circ\text{C}$  with shaking in Luria Bertani broth overnight. The preculture was diluted 50-fold and allowed to continue for another 3–4 h, until the  $\text{OD}_{600\text{nm}}$  had reached 0.6–1.0 [15]. The culture was then diluted to  $10^6 \text{ CFU mL}^{-1}$  and aliquoted in a sterile 96-well plate. PVP/PB NPs were added at different concentrations and the wells were irradiated at 810 or 980 nm. Afterwards, the resistant bacteria were counted on LB agar.

The *S. aureus* ATCC25923 and MRSA ATCC43300 strains were grown at  $37^\circ\text{C}$  with shaking in Brain-heart-infusion (BHI) broth for 3–4 h until the  $\text{OD}_{600\text{nm}}$  reached 0.3–0.5. The cultures were aliquoted in a sterile 96-well plate at  $10^6 \text{ CFU mL}^{-1}$ . PVP/PB NPs were

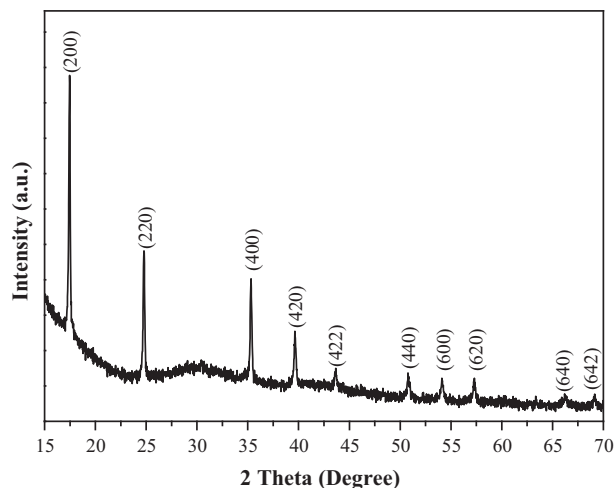


Fig. 1. XRD pattern of PVP/PB nanoparticles.

added at different concentrations and the wells were irradiated at 810 or 980 nm. Following this treatment, bacteria were plated and the resistant ones were counted on BHI agar.

## 3. Results and discussion

The PVP/PB NPs investigated in this work were synthesized according to [25]. The PVP/PB NPs are highly stable in aqueous solution without any apparent precipitation or aggregation for several months at room temperature.

Fig. 1 depicts the XRD pattern of the as-obtained blue powder. It consists of some sharp peaks at  $17.6^\circ$  (2 0 0),  $24.8^\circ$  (2 2 0),  $35.3^\circ$  (4 0 0),  $39.6^\circ$  (4 2 0),  $43.7^\circ$  (4 2 2),  $50.9^\circ$  (4 4 0),  $54.1^\circ$  (6 0 0),  $57.3^\circ$  (6 2 0),  $66.2^\circ$  (6 4 0), and  $69.3^\circ$  (6 4 2), which can be indexed to face-centered cubic crystallographic phase of PB (ICDD File No. 52-1907). No additional unassigned peak was detected.

Transmission electron microscopy (TEM) imaging reveals that the PB NPs are mainly in the form of uniform nanocubes  $\sim 70$ – $90 \text{ nm}$  in size (Fig. 2A).

Selective area electron diffraction (SAED) pattern (see the inset of Fig. 2A) on a single nanocube comprises some diffraction rings, indicating the polycrystallinity of the material. These rings could be indexed to different crystal planes of the cubic phase of PB. High resolution TEM image taken on the edge of a single nanocube further confirms the polycrystallinity; some grains,  $\sim 10 \text{ nm}$  or smaller in size, were imaged. The observed  $d$ -spacing of  $\sim 0.50$  and  $0.31 \text{ nm}$  agrees well with the lattice spacing of the (2 0 0) and (2 2 0) planes of PB, respectively (Fig. 2B).

The UV–vis spectra of aqueous solutions of PVP/PB NPs display strong light absorption in the range of 500–1000 nm, providing a possibility to be exploited for bacteria photothermal ablation under NIR irradiation (Fig. 3). The absorption of PVP/PB NPs in this region is attributed to the charge transfer transition between Fe(II) and Fe(III) in PB NPs.

The photothermal heating capacity of PVP/PB NPs suspensions was determined by measuring the temperature changes under NIR irradiation at 810 and 980 nm using a continuous wave laser. For the same concentration, the final solution temperature reached was  $\sim 10^\circ\text{C}$  higher for the irradiation at 810 nm than that at 980 nm (see Fig. 4).

In a control experiment, we have irradiated aqueous solutions of PVP at 250 and  $500 \mu\text{g mL}^{-1}$  at 810 nm ( $1 \text{ W cm}^{-2}$ ) for 10 min (Fig. S2). Under these experimental conditions, the final temperature reached was comparable to that obtained using only water (in absence of PVP). The results clearly indicate that the observed photothermal effect was due to PB NPs.

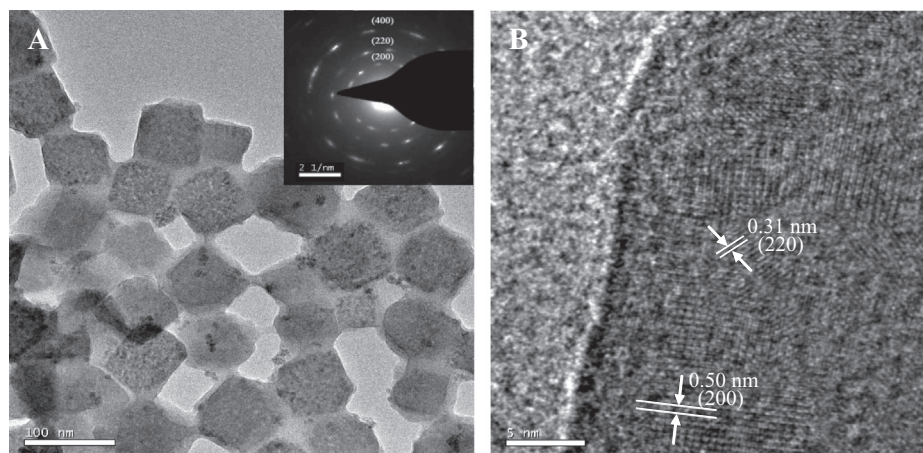


Fig. 2. TEM (A) and HRTEM (B) of the PVP/PB NPs. The inset in (A) corresponds to the selective area electron diffraction (SAED) pattern.

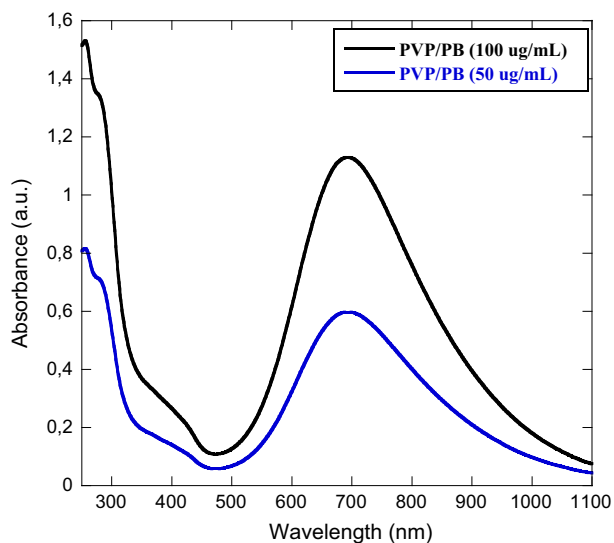


Fig. 3. UV-vis absorption spectra of the PVP/PB NPs in water at two different concentrations.

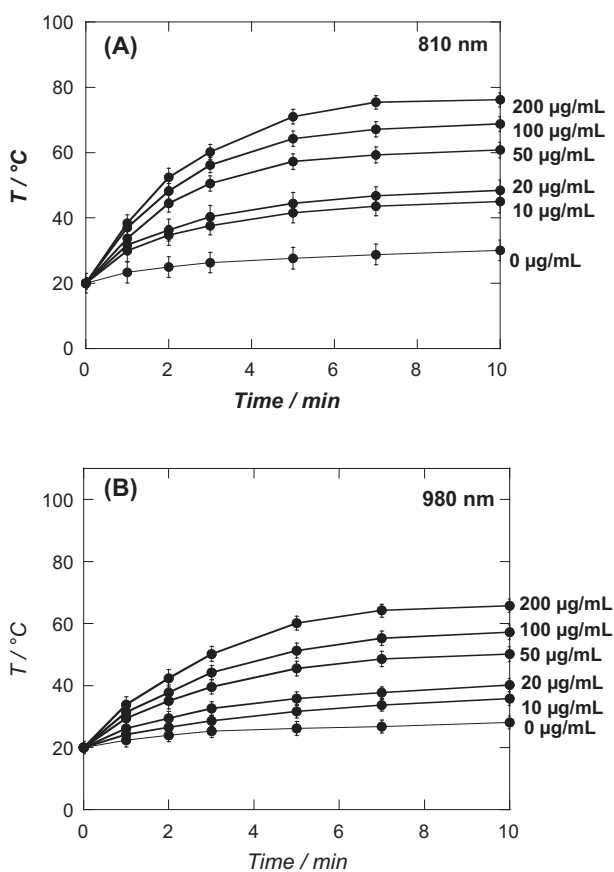


Fig. 4. Photothermal heating curves of PVP/PB NPs suspensions under NIR illumination using a continuous laser at (A) 810 nm and (B) 980 nm. Laser power:  $1 \text{ W cm}^{-2}$ .

Prior to investigating the photothermal effect on bacteria, the cytotoxicity of PVP/PB NPs was evaluated using HeLa and Caco-2 cell lines (Figs. 5 and S1). PVP/PB NPs showed low cell growth inhibition for both cell lines up to  $200 \mu\text{g mL}^{-1}$ . The *in vitro* cytotoxicity of PVP/PB NPs under irradiation by NIR was additionally determined. HeLa cells were incubated with increasing

concentrations of PVP/PB NPs and irradiated for 10 min at 810 or 980 nm for 10 min at  $1 \text{ W cm}^{-2}$ . As shown in Fig. 5, a dose dependent cytotoxicity was observed. A PVP/PB NPs concentration of  $25 \mu\text{g mL}^{-1}$  displays 30% cell viability when irradiated at 810 nm. This is in sharp contrast to irradiation at a longer wavelength (980 nm), where no significant decrease in cell viability was observed up to a NP concentration of  $50 \mu\text{g mL}^{-1}$ . The higher cell killing ability at 810 nm was attributed to the better photothermal properties achieved at this wavelength.

To exclude cell killing under laser illumination, HeLa cells were irradiated at 810 nm ( $1 \text{ W cm}^{-2}$ ) as a function of time in absence of PVP/PB NPs (Fig. S3). Up to 25 min irradiation, the cell viability was not affected, suggesting that under our experimental conditions HeLa cells were not sensitive to laser irradiation; this also indicates that the observed cell killing in presence of PVP/PB NPs was due to photothermal effect.

Furthermore, we have examined the ability of PVP/PB NPs to generate singlet oxygen ( $^1\text{O}_2$ ) under 810 or 980 nm irradiation. Singlet oxygen generation was monitored through the chemical oxidation of an aqueous solution of 9,10-anthracenediylbis(methylene)dimalonic acid (ABDA) ( $10 \mu\text{M}$ ) in the presence of PVP/PB NPs ( $100 \mu\text{g mL}^{-1}$ ). Fig. S4 depicts the UV-vis absorption spectra of an aqueous solution of (ABDA) ( $10 \mu\text{M}$ ) and PVP/PB NPs ( $100 \mu\text{g mL}^{-1}$ ) before and after irradiation at  $1 \text{ W cm}^{-2}$  for 10 min at 810 or 980 nm. The results indicate no  $^1\text{O}_2$  generation under these experimental conditions, confirming that cell/bacteria killing was mainly caused by a photothermal effect.

The efficiency of PVP/PB NPs to ablate pathogens was investigated by mixing a suspension of *E. coli* ( $10^6 \text{ CFU mL}^{-1}$ ) with PVP/PB NPs at different concentrations followed by irradiation of the suspension for 10 min at 810 nm or 980 nm ( $1 \text{ W cm}^{-2}$ ) and performing a proliferation assay. Virulent strains of *E. coli*, associated with urinary tract infection (UTIs), was photothermally treated as recurrent urinary tract infections caused by *E. coli* UTI has shown to significantly reduce the effect of ciprofloxacin treatments, with a major threat for the development of antibiotic resistance.

As seen in Fig. 6, photothermal treatment of *E. coli* UTI with  $100 \mu\text{g mL}^{-1}$  of PVP/PB NPs at  $1 \text{ W cm}^{-2}$  for 10 min completely destroyed the pathogens regardless if 810 or 980 nm laser irradiation was used. It is worthy to notice that a PVP/PB NPs concentration of  $50 \mu\text{g mL}^{-1}$  resulted in a 5-log reduction of *E. coli* strains upon laser irradiation at 810 or 980 nm, while at this concentration range irradiation at 980 nm exhibited only a slight decrease of HeLa cell viability (Fig. 5). It is well known that a good antibacterial compound should selectively target bacteria over mammalian cells; the combination of PB particles with laser irradiation at 980 nm should be a way in this direction. Herein the benefit of PVP/PB NPs over other photothermal agents used for the ablation of pathogens [26,27], is associated with the low laser power used, making the approach more attractive.

Furthermore, we validated the concept of PTT at 980 nm using PVP/PB NPs on other model pathogens. Among the several known *Staphylococcus* species, methicillin-resistant *S. aureus* (MRSA) is a pathogen of high clinical importance as it is known to be resistant to a wide range of antibiotics, making its eradication a real challenge [28]. Fig. 7 shows that these antibiotic resistant bacteria are completely killed after 10 min irradiation at 980 nm using a PVP/PB NPs concentration as low as  $20 \mu\text{g mL}^{-1}$ . Conversely to *S. aureus* ATCC25923, where the viability decreased by almost 6  $\log_{10}$  between PVP/PB NPs concentration of 10 and  $15 \mu\text{g mL}^{-1}$ , the change in viability of MRSA strain decreases steadily upon increasing the particle concentration under otherwise similar conditions.

In addition, a major difference was observed between *E. coli* UTI89 and antibiotic-resistant *E. coli* ESBL using PVP/PB NPs PTT treatment. A much higher PVP/PB NPs concentration ( $>50 \mu\text{g mL}^{-1}$ )

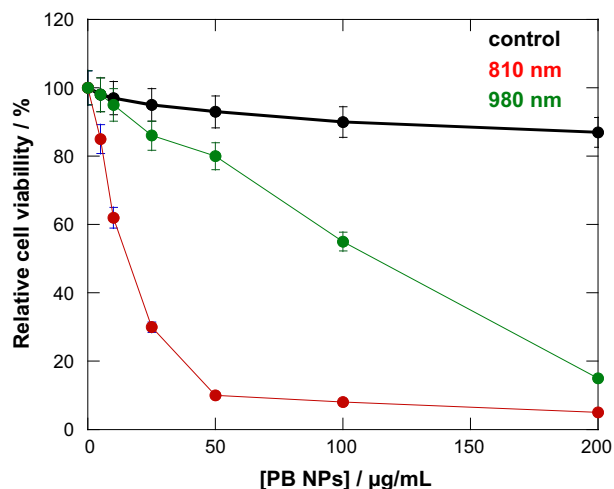


**Fig. 5.** Relative cell viability of HeLa cells as a function of PVP/PB NPs concentration (cell viability was evaluated using the CCK-8 assay, where the absorbance at 450 nm is measured using a microplate reader) without irradiation (●), irradiation at 810 nm for 10 min at  $1 \text{ W cm}^{-2}$  (●) and irradiation at 980 nm for 10 min at  $1 \text{ W cm}^{-2}$  (●).

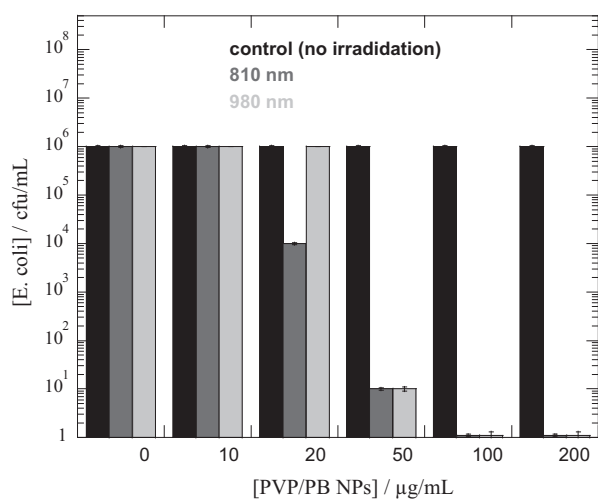


**Fig. 6.** Treatment of *E. coli* UTI89 ( $10^6 \text{ CFU mL}^{-1}$ ) with different concentrations of PVP/PB NPs using a continuous wave laser at 810 or 980 nm for 10 min at  $1 \text{ W cm}^{-2}$ .

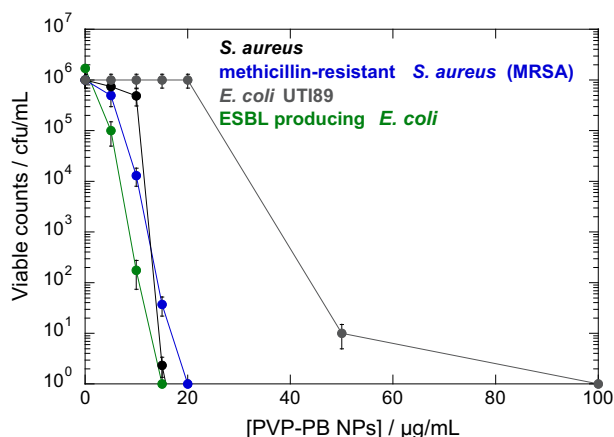


**Fig. 7.** Influence of the PVP/PB NPs concentration on the photothermal treatment efficiency of Gram-positive (*S. aureus* and MRSA) and Gram-negative bacteria (*E. coli* UTI89 and ESBL producing *E. coli*) ( $10^6 \text{ CFU mL}^{-1}$ ) under laser irradiation at 980 nm for 10 min at  $1 \text{ W cm}^{-2}$ .

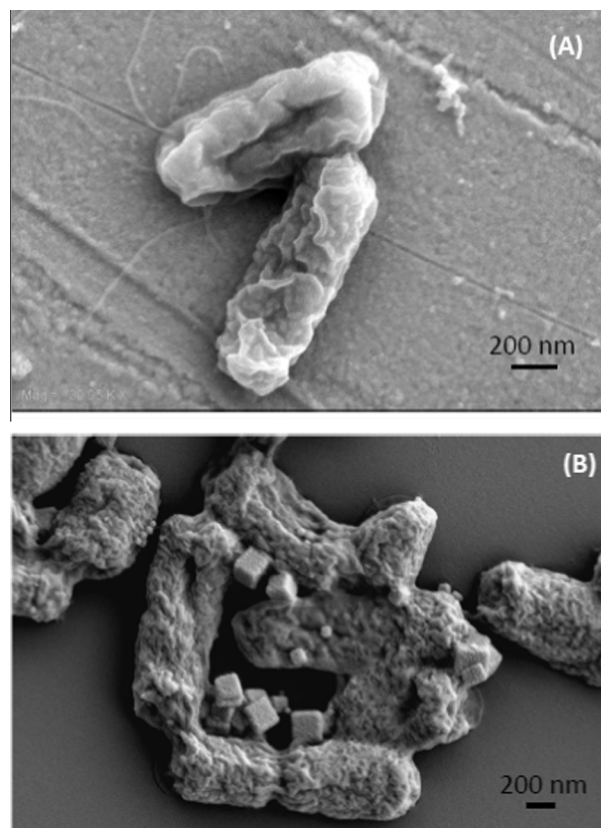


**Fig. 8.** SEM image of *E. coli* UTI89 before (A) and (B) after irradiation in the presence of PVP/PB NPs using a continuous wave laser at 980 nm for 10 min (laser power =  $1 \text{ W cm}^{-2}$ ).

was needed for a total eradication of the pathogen, while the ESBL producing *E. coli* strain showed similar behavior as *S. aureus*.

Finally, we used SEM imaging before and after irradiation at 980 nm to gain a better understanding on the mechanism of bacteria eradication. Fig. 8 clearly reveals that the PVP/PB NPs aggregate in the close vicinity of the bacteria without any evidence for nanoparticles entry inside the bacteria. The result suggests that bacteria eradication takes place through effective heating of the medium, leading to destruction of the cell membrane (presence of holes in the bacteria membrane as seen in Fig. 8).

#### 4. Conclusion

In conclusion, we have demonstrated that PVP-coated Prussian blue nanoparticles (PVP/PB NPs) could serve as efficient photothermal agents under NIR (810 or 980 nm) irradiation for efficient ablation of virulent and antibiotic resistant pathogens, including virulent strains of *E. coli* associated with urinary tract infection, and methicillin-resistant *S. aureus*. More interestingly, PVP/PB NPs derived PTT enabled pathogen killing in a concentration dependent manner using 980 nm NIR laser power of  $1 \text{ W cm}^{-2}$ . An important finding is that by choosing an appropriate PVP/PB NPs concentration ( $<50 \mu\text{g mL}^{-1}$ ) and 980 nm irradiation wavelength selective treatment of bacteria over mammalian cells can be achieved. Finally, by choosing appropriate ligands it will be possible to target specifically bacteria receptors in infected tissues for efficient photothermal therapy.

#### Acknowledgements

R.B. and S.S. gratefully acknowledge financial support from the Centre National de la Recherche Scientifique (CNRS), the University

Lille 1 and Nord-Pas-de Calais region. S.S thanks the Institut Universitaire de France (IUF) for financial support. G.-H.P. is grateful to financial support from National Natural Science Foundation of China (Grants No. 51202019 and 51402284) and Twelfth Five-Year Plan of The Education Department of Jilin Province for Science and Technology Study (Grant no. 2014-266).

## Appendix A. Supplementary material

Supplementary data associated with this article can be found, in the online version, at <http://dx.doi.org/10.1016/j.jcis.2016.07.002>.

## References

- [1] N.W. Schmidt, S. Deshayes, S. Hawker, A. Blacker, A.M. Kasko, G.C.L. Wong, Engineering persister-specific antibiotics with synergistic antimicrobial functions, *ACS Nano* 8 (2014) 8786–8793.
- [2] S.G. Bell, Antibiotic resistance: is the end of an era near?, *Neonatal Netw.* 22 (2003) 47–54.
- [3] N.K. Petty, N.L. Ben Zakour, M. Stanton-Cook, E. Skippington, M. Totsika, B.M. Forde, M.D. Phan, D. Gomes Moriel, K.M. Peters, M. Davies, B.A. Rogers, G. Dougan, J. Rodriguez-Bano, A. Pascual, J.D. Pitout, M. Upton, D.L. Paterson, T.R. Walsh, M.A. Schembri, S.A. Beatson, Global dissemination of a multidrug resistant *Escherichia coli* clone, *Proc. Nat. Acad. Sci. USA* 111 (2014) 5694–5699.
- [4] S.M. Dizaj, F. Lotfipour, M. Barzegar-Jalali, M.H. Zarrintan, K. Adibkia, Antimicrobial activity of the metals and metal oxide nanoparticles, *Mater. Sci. Eng. C* 44 (2014) 278–284.
- [5] A.J. Huh, Y.J. Kwon, “Nanoantibiotics”: a new paradigm for treating infectious diseases using nanomaterials in the antibiotics resistant era, *J. Control. Release* 156 (2011) 128–145.
- [6] J. Wehling, R. Dringer, R.N. Zare, M. Maas, K. Rezwan, Bactericidal activity of partially oxidized nanodiamonds, *ACS Nano* 8 (2014) 6475–6483.
- [7] V. Turcheniuk, V. Raks, R. Issa, I.R. Cooper, P.J. Cragg, R. Jijie, N. Dumitrescu, L.I. Mikhalovska, A. Battas, V. Zaitsev, R. Boukherroub, S. Szunerits, Antimicrobial activity of menthol modified nanodiamond particles, *Diamond Relat. Mater.* 57 (2015) 2–8.
- [8] X. Dai, Z. Fan, Y. Lu, P.C. Ray, Multifunctional nanoplatfoms for targeted multidrug-resistant-bacteria theranostic applications, *ACS Appl. Mater. Interfaces* 5 (2013) 11348–11354.
- [9] C.A. Strassert, M. Otter, R.Q. Albuquerque, A. Hone, Y. Vida, B. Maier, L. De Cola, Photoactive hybrid nanomaterial for targeting, labeling, and killing antibiotic-resistant bacteria, *Angew. Chem. Int. Ed.* 48 (2009) 7928–7931.
- [10] K.-H. Choi, H.-L. Lee, B.J. Park, K.-K. Wang, E.P. Shin, J.-C. Park, Y.K. Kim, M.-K. Oh, Y.-R. Kim, Photosensitizer and vancomycin-conjugated novel multifunctional magnetic particles as photoinactivation agents for selective killing of pathogenic bacteria, *Chem. Commun.* 48 (2012) 4591–4593.
- [11] R.A. Weissleder, A clearer vision for *in vivo* imaging, *Nat. Biotechnol.* 19 (2001) 316–317.
- [12] Y.M. Bae, Y.I. Park, S.H. Nam, J.H. Kim, K. Lee, H.M. Kim, B. Yoo, J.S. Choi, K.T. Lee, T. Hyeon, Y.D. Suh, Endocytosis, intracellular transport, and exocytosis of lanthanide-doped upconverting nanoparticles in single living cells, *Biomaterials* 33 (2012) 9080–9086.
- [13] S.H. Nam, Y.M. Bae, B.J. Park, J.H. Kim, H.M. Kim, J.S. Choi, K.T. Lee, T. Hyeon, Y. D. Suh, Long-term real-time tracking of lanthanide ion doped upconverting nanoparticles in living cells, *Angew. Chem. Int. Ed.* 50 (2011) 6093–6097.
- [14] K.E. Sivick, H.L.T. Mobley, Waging war against uropathogenic *Escherichia coli*: winning back the urinary tract, *Infect. Immun.* 78 (2010) 568–585.
- [15] A.K. Al Atya, K. Drider-Hadiouche, A. Vachée, D. Drider, Potentialization of  $\beta$ -lactams with colistin: in case of extended spectrum  $\beta$ -lactamase producing *Escherichia coli* strains isolated from children with urinary infections, *Res. Microbiol.* <http://dx.doi.org/10.1016/j.resmic.2015.12.002>.
- [16] C. Liu, A. Bayer, S.E. Cosgrove, R.S. Daum, S.K. Fridkin, R.J. Gorwitz, S.L. Kaplan, A.W. Karchmer, D.P. Levine, B.E. Murray, M.J. Rybak, D.A. Talan, H.F. Chambers, Clinical practice guidelines by the infectious diseases society of America for the treatment of methicillin-resistant *Staphylococcus aureus* infections in adults and children: executive summary, *Clin. Inf. Dis.* 52 (2010) 285–292.
- [17] W. Zhu, K. Liu, X. Sun, X. Wang, Y. Li, L. Cheng, Z. Liu, Mn<sup>2+</sup>-doped Prussian blue nanocubes for bimodal imaging and photothermal therapy with enhanced performance, *ACS Appl. Mater. Interfaces* 7 (2015) 11575–11582.
- [18] H.A. Hoffman, L. Chakrabarti, M.F. Dumont, A.D. Sandler, R. Fernandes, Prussian blue nanoparticles for laser-induced photothermal therapy of tumors, *RSC Adv.* 4 (2014) 29729–29734.
- [19] G. Fu, W. Liu, Y. Li, Y. Jin, L. Jiang, X. Liang, S. Feng, Z. Dai, Magnetic Prussian blue nanoparticles for targeted photothermal therapy under magnetic resonance imaging guidance, *Bioconjugate Chem.* 25 (2014) 1655–1663.
- [20] Z. Li, Y. Zeng, D. Zhang, M. Wu, L. Wu, A. Huang, H. Yang, X. Liu, J. Liu, Glypican-3 antibody functionalized Prussian blue nanoparticles for targeted MR imaging and photothermal therapy of hepatocellular carcinoma, *J. Mater. Chem. B* 2 (2014) 3686–3696.
- [21] G. Fu, W. Liu, S. Feng, X. Yue, Prussian blue nanoparticles operate as a new generation of photothermal ablation agents for cancer therapy, *Chem. Commun.* 48 (2012) 11567–11569.
- [22] P. Xue, J. Bao, Y. Wu, Y. Zhang, Y. Kang, Magnetic Prussian blue nanoparticles for combined enzyme-responsive drug release and photothermal therapy, *RSC Adv.* 5 (2015) 28401–28409.
- [23] Y. Li, C.H. Li, D.R. Talham, One-step synthesis of gradient gadolinium ironhexacyanoferrate nanoparticles: a new particle design easily combining MRI contrast and photothermal therapy, *Nanoscale* 7 (2015) 5209–5216.
- [24] P. Xue, K.K.Y. Cheong, Y. Wu, Y. Kang, An in-vitro study of enzyme-responsive Prussian blue nanoparticles for combined tumor chemotherapy and photothermal therapy, *Colloids Surf. B: Biointerfaces* 125 (2015) 277–283.
- [25] H. Ming, N.L.K. Torad, Y.-D. Chiang, K.C.-W. Wu, Y. Yamauchi, Size- and shape-controlled synthesis of Prussian blue nanoparticles by a polyvinylpyrrolidone-assisted crystallization process, *CrystEngComm* 14 (2012) 3387–3396.
- [26] K. Turcheniuk, C.-H. Hage, J. Spadavecchia, A.Y. Serrano, I. Larroulet, A. Pesquera, A. Zurutuza, M.G. Pisfil, L. Heliot, J. Bouckaert, R. Boukherroub, S. Szunerits, Plasmonic photothermal destruction of uropathogenic *E. coli* with reduced graphene oxide and core/shell nanocomposites of gold nanorods/reduced graphene oxide, *J. Mater. Chem. B* 3 (2015) 375–386.
- [27] M.-C. Wu, A.R. Deokar, J.-H. Liao, P.-Y. Shih, Y.-C. Ling, Graphene-based photothermal agent for rapid and effective killing of bacteria, *ACS Nano* 7 (2013) 1281–1290.
- [28] G. Taubes, The bacteria fight back, *Science* 321 (2008) 356–361.